ICSV13 - Vienna
The Thirteenth International Congress on Sound and Vibration
Vienna, Austria, July 2-6, 2006

# STUDY ON EXPERIMENTAL APPLICATION OF WIA AND COMPARISON WITH SEA, WIA AND ESEA

J. Javier Bayod *[1], Toru Yamazaki [1], and Minoru Kamata[2]

[1]University of Tokyo Dep. of Mechanical Engineering,
7-3-1 Hongo, Bunkyo-ku, Tokyo 113-8654, Japan
[2]Kanagawa University, Dep. of Mechanical Engineering,
3-27-1 Rokkakubashi, Kanagawaku, Yokohama 221-8686, Japan
Javier@sl.t.u-tokyo.ac.jp

## Abstract

This paper describes an application of Experimental Wave Intensity Analysis technique (EWIA) to predict the vibration energy of a simple plate system and a car dash-floor model. EWIA uses coupling loss factors (CLF) and internal loss factors (ILF) obtained experimentally through the power injection method. The directional dependency of the energy transmission, required in WIA, is introduced by deriving a transmission coefficient $\tau(\theta)$ for each subsystem at each frequency. WIA and EWIA energy distributions are compared using the L-shape plate system results. Then energy predictions are compared with measured energies and Experimental SEA (ESEA) predictions for the car dash-floor system. The results show that EWIA can be applied to complex systems without additional measuring or modeling effort compared to WIA or ESEA.

## INTRODUCTION

Vibration analysis is of great interest in many engineering applications since it can help to reduce noise levels, improve systems safety or accuracy of high precision machinery for example. But low and high frequency vibration analysis present a number of restrictions that limit their applications. The most popular method for low frequency analysis is the Finite Element Method (FEM) [7]. The computational time required by an FEM calculation is in great part determined by the size of the finite elements. As frequency increases the wavelength decreases and smaller elements are necessary, consequently increasing their numbers and the calculation time making the simulation more and more expensive.

In the high frequencies the most popular method is Statistical Energy Analysis (SEA) or its experimental application called Experimental SEA (ESEA). Statistical methods greatly improve the computational efficiency but these methods are based on a number of assumptions needed to ensure accurate predictions. As frequency becomes lower it is more difficult for the SEA subsystems to satisfy those assumptions and as a result the prediction may become inaccurate.

It is therefore important to improve the restrictions of these methods in order to extend their applicability. This study aims to extend the WIA method, which is an improvement of the SEA method in high frequency ranges, by farther researching an experimental application EWIA proposed in ref. [3]. In this paper the method is applied to more complex systems while avoiding the tedious experiments involved in the determination of the required energy intensity vectors. In this way EWIA keeps the simplicity characteristic of SEA, ESEA and WIA.

## OUTLINE OF WAVE INTENSITY ANALYSIS

### WIA method

In contrast to SEA, WIA takes into account the direction of the energy transmitted at subsystem's boundaries relaxing the assumption of highly diffuse field [9,10]. The formulation is based on the SEA power balance equation but it describes the problem from a fully wave point of view while SEA is based on a time domain view.

In WIA the power terms of the power balance equation are described as energy carried by waves that travel in different directions. Thus, the angle of propagation of the energy is also introduced as a variable. To express the coupling terms in the power balance equation WIA uses directionally dependent transmission coefficients $\tau(\theta)$. The WIA power balance equation for a wave type *j* is [9,10]

$$P_j^{in}(\theta,\omega) = P_j^{diss}(\theta,\omega) + P_j^{co}(\theta,\omega) - P_j^{ci}(\theta,\omega) \tag{1}$$

Where $P_j^{in}$ is the power input, $P_j^{diss}$ is the power dissipated, $P_j^{co}$ and $P_j^{ci}$ represent output and input power at boundaries, $\omega$ is the mean frequency and $\theta$ is the direction of propagation of wave *j*. *j* corresponds to the type of wave considered (flexural, etc).

The power terms of Eq. (1) are expanded in the space domain and powers are written in terms of energies and coupling terms [9,10] then, for multiple subsystems the following matrix equation is obtained where coupling terms and energies are separated in the C and $\widehat{E}$ matrices respectively.

$$\boldsymbol{C}\widehat{\boldsymbol{E}} = \boldsymbol{P} \tag{2}$$

$$P_{jp} = \int_0^{2\pi} P_j^{in}(\theta,\omega) N_p^j(\theta)\, d\theta \tag{3}$$

$$C_{jp,is} = \delta_{ij} \left\{ \omega \eta_j v_j \int_0^{2\pi} N_p^j(\theta) N_s^i(\theta) d\theta + (\omega / 2\pi c_j) \sum_k L_k \int_{\Theta k} N_p^j(\theta) N_s^i(\theta) \cos(\theta + \pi/2 - \psi_k) d\theta \right\}$$
$$- (\omega / 2\pi c_j) \sum_m L_m \int_{\Theta_m} N_p^j(\theta) N_s^i(\phi_{mi}) \cos(\theta + \pi/2 - \psi_m) \tau_{ij}^m (\phi_{mi} + \pi/2 - \psi_m) d\theta \tag{4}$$

Where $\widehat{E}$ represents the $E_{jp} / v_j$ coefficients $N_p^j(\theta)$ and $N_s^j(\theta)$ are the Fourier terms $\Theta_m$ and $\Theta_k$ are the angular ranges of input and output boundaries.

## EXPERIMENTAL WAVE INTENSITY ANALYSIS (EWIA)

A simplified EWIA application is derived in this section considering only flexural waves for simplicity. The term ‘simplified’ indicates that the intention is also to avoid the tedious experiments involved in the determination of energy intensity vectors so that the simplicity characteristic of SEA, ESEA and WIA is also preserved for EWIA.

This paper investigates the possibility of using ESEA experimental data; then adjust the coupling terms with scaling constants derived from the relationship between the experimental CLFs and the theoretical $\tau(\theta)$. Thus, assuming that the averaged energy in the subsystems corresponds to the measured energy and its distribution at the boundaries follows a theoretical model. This is justified by considering that the transmission of energy at regular boundaries is similar to its theoretical model at least at a short distance from the boundary. These types of boundaries tend to promote a more diffuse field while more irregular boundaries, more difficult to compare with theoretical models, contribute to more non-diffuse fields and therefore a non-diffuse model of these may suffice for an enough accurate prediction.

The advantage of this EWIA application is the possibility of improving the accuracy of ESEA results without increasing the complexity of the procedures.

### Estimation of transmission coefficients from ESEA data

In this section $\tau(\theta)$ is estimated from typical SEA experimental data based on the relationship between the CLFs at a boundary and its theoretical $\tau(\theta)$.

$$\eta_{ji}^m = (L_m c_{gj} / \omega A_j \pi) \left\langle \tau_{ji}^m \right\rangle \tag{5}$$

$$\left\langle \tau_{ji}^m \right\rangle = \frac{1}{2} \int_{\Theta_m} \cos(\theta) \tau(\theta) d\theta \tag{6}$$

Where $L_m$ is the length of the connecting boundary, $c_{gj}$ is the group velocity, $A_j$ is the area of subsystem *j*, $\left\langle \tau_{ji}^m \right\rangle$ is the angular averaged transmission coefficient from *j* to *i* at boundary *m* for the corresponding wave type and $\Theta_m$ the angular range of boundary *m*.

The actual averaged energy transmitted between subsystems often differs from its theoretical model due to connection or material irregularities; by using a constant value the theoretical model is scaled so that its averaged energy matches the averaged energy measured in the experiments while its angular distribution will follow the corresponding theoretical pattern given by τ ( θ ), assuming that the irregularities near the connection do not greatly affect the angular distribution of energy.

The energies exchanged in SEA can be compared with the angular averaged energies exchanged in WIA what is done considering only the first Fourier term in each Fourier series [9,10]. Thus the ratio between the transmitted energies in SEA and angular averaged of transmitted energies in WIA is

$$\frac{E_{ij}}{E_{ji}} = \frac{\omega\eta_{ij}^{m,e}\left\langle E_i \right\rangle_e}{\omega\eta_{ji}^{m,e}\left\langle E_j \right\rangle_e} = \frac{\omega\eta_{ij}^{m,t}\left\langle E_i^{wia} \right\rangle_t}{\omega\eta_{ji}^{m,t}\left\langle E_j^{wia} \right\rangle_t} \tag{7}$$

Where $E_{ji}$ and $E_{ij}$ are the energies exchanged between subsystems, $\left\langle E_j \right\rangle_e$ and. $\left\langle E_j^{wia} \right\rangle_t$ are respectively the energy of subsystem *j* measured experimentally and its energy calculated theoretically by WIA using a single Fourier term. The terms $\eta_{ji}^{m,e}$ and $\eta_{ji}^{m,t}$ are respectively the CLFs of boundary *m* estimated experimentally (ESEA CLFs) and the ones estimated theoretically from material properties. In Eq.(7) the ratios of transmitted energy of ESEA and diffuse-field WIA should be same; in practice this can be ensured by using a constant scale factor, *Cnst,* to adjust the coupling coefficients

$$\frac{\eta_{ij}^{m,e}}{\eta_{ji}^{m,e}} = Cnst\,\frac{\eta_{ij}^{m,t}}{\eta_{ji}^{m,t}} \quad ; \quad Cnst = \frac{\eta_{ji}^{m,e}\eta_{ij}^{m,t}}{\eta_{ji}^{m,t}\eta_{ij}^{m,e}} \tag{8), (9}$$

**Relationship between transmission coefficient and scaling constants**

CLFs are estimated from experiments using for example the power injection method and an ‘experimental’ angular average of τ ( θ ), $\left\langle \tau_{ji}^{m} \right\rangle_e$, is estimated using Eq.(5) and Eq.(6). The theoretical average of τ ( θ ), $\left\langle \tau_{ji}^{m} \right\rangle_t$ ,can be calculated using material data [4]. Therefore combining Eq.(5), (6), (8) and (9) results on

$$Cnst_{ji} = \left\langle \tau_{ji}^{m} \right\rangle_e / \left\langle \tau_{ji}^{m} \right\rangle_t \tag{10}$$

If this constant is applied to the theoretical τ ( θ ) at each angle of transmission, the result is a distribution of energy which follows the theoretical model but which average matches the average of actual measured energy in the experiments.

## APPLICATION OF EWIA AND COMPARISON WITH ESEA

### Application to simple plate structure

This system consists of a L-shaped steel panel with Young's modulus $E$=1.9995x10$^{11}$ N/m$^2$, Poison's ratio=0.35 and density $\rho$ =7834.6 Kg/m$^3$. The lengths are: Plate_1 = 0.5m and Plate_2 = 0.4m. The widths are 0.35m. Power is input in subsystem #1. Experimental data (ILFs and CLFs) are obtained using the power injection method.

The top sub-plots of Fig.(1) show that the shape of energy distribution in a EWIA model is same as WIA but takes different values at each angle of transmission. These sub-plots correspond to the Fourier series of the energy at each subsystem for WIA and EWIA estimations. The bottom sub-plot of Fig.(1) shows the influence that this scaling has in the energy predictions and distributions inside the subsystems. Again the distribution have same pattern for both methods but with different values at each angle.

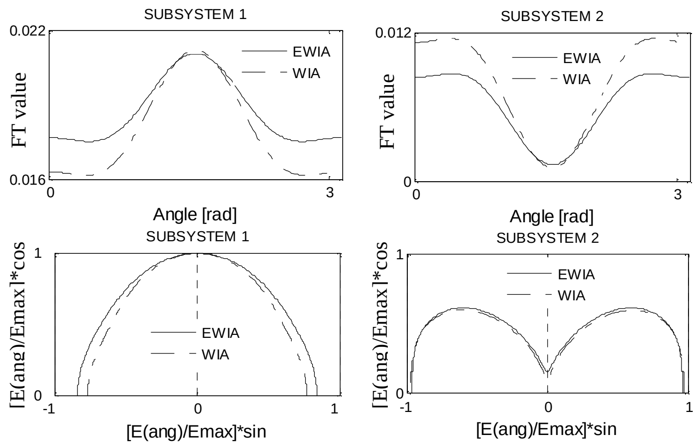


*Figure 1 Top: Fourier series for WIA and EWIA models*
*Figure 1 Bottom: Subsystems energy distribution for same number of Fourier terms*

It is also found that the accuracy of EWIA predictions depends on the number of Fourier terms in the same way as in WIA and for simple plate systems the minimum number of terms to obtain enough accurate energy predictions is 3 or 5. Fig.(2) shows the difference on the EWIA prediction of energy levels using different number of Fourier terms. The difference between the Fourier series, Fig(2) top subplots, is not important when comparing the 3-terms and 15-terms distributions although increases as the transmission angle approaches pi/2rad. The difference of the energy-prediction ratio between these cases is about 0.08dB. When comparing the energy distributions on the subsystems, Fig(2) bottom subplots, both distributions are very close to each other with the larger discrepancy at pi/2rad in second subsystem. Therefore, in this case only 3 terms may suffice for a good prediction as in WIA. Fig.2 also compares the Fourier series and energy distributions when using 30 Fourier terms. The curves corresponding to this case are very close to the 15-terms curves and cannot be distinguished. The difference between the 15-terms and 30-terms predictions is about $2E^{-7}$dB what indicates a quick convergence of the results. Fig.(3) illustrates a comparison of energy predictions between SEA, ESEA, WIA and EWIA.

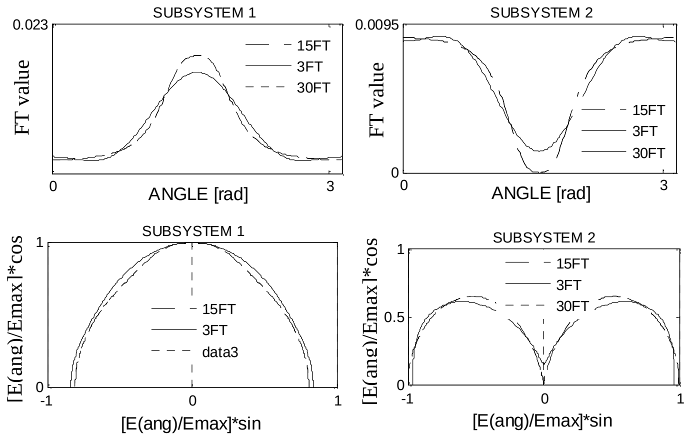


*Figure 2 Top: Fourier series for EWIA model for different number of Fourier terms*
*Figure 2 Bottom: EWIA subsystems energy distribution for different number of Fourier terms*

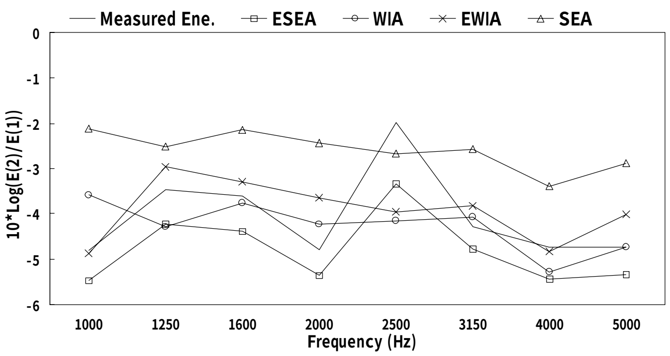


*Figure 3: Comparison between measured data, SEA(experimental ILF), ESEA, WIA (experimental ILF) and EWIA*

## Application to car dash-floor system

This system, as shown in Fig.(4), was divided into eight subsystems all of them considered rectangular. Fig.5 shows a comparison between the ESEA, EWIA energy predictions and measured data for this model. Since energy is input in subsystem #1 the energy field in this component can be considered diffuse and therefore ESEA and EWIA estimations should be very similar. This behaviour is observed in the first subsystem results, which correspond to the top plot on the left column. Also the directly connected subsystems, #2, #3 and #4 could be expected to be still quite diffuse since there is just a single boundary between these and subsystem #1 and therefore energy filtering may not have great influence. The following plots on the left column of Fig.5 confirm this; the EWIA and ESEA results are very close for all the frequency range. Increasing the number of boundaries between subsystems increases the energy filtering and therefore the influence on the prediction becomes more important and the WIA estimation should improve respect to SEA. This point is highlighted in the four plots on the right column of Fig.5, which correspond to the last four subsystems of the model. This plots show that EWIA can improve the ESEA results at most frequencies as the distance from the power source subsystem, #1, is increased. This is confirmed by observing that the better predictions correspond to the last subsystem, #8, which is ‘one boundary farther’ than subsystems #5, #6 and #7 where the trend of the prediction is already good. Accuracy also increases with frequency as expected from SEA or WIA basic formulation due mainly to higher modal overlap.

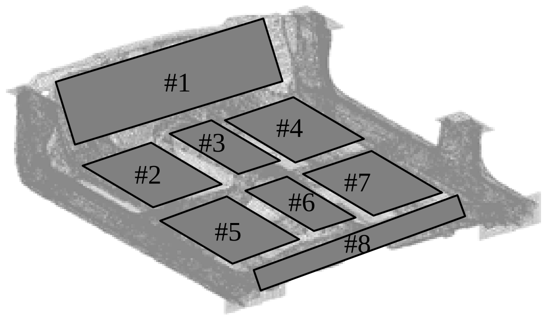


*Figure 4: 8-subsystems SEA model of car Dash-floor cut model*

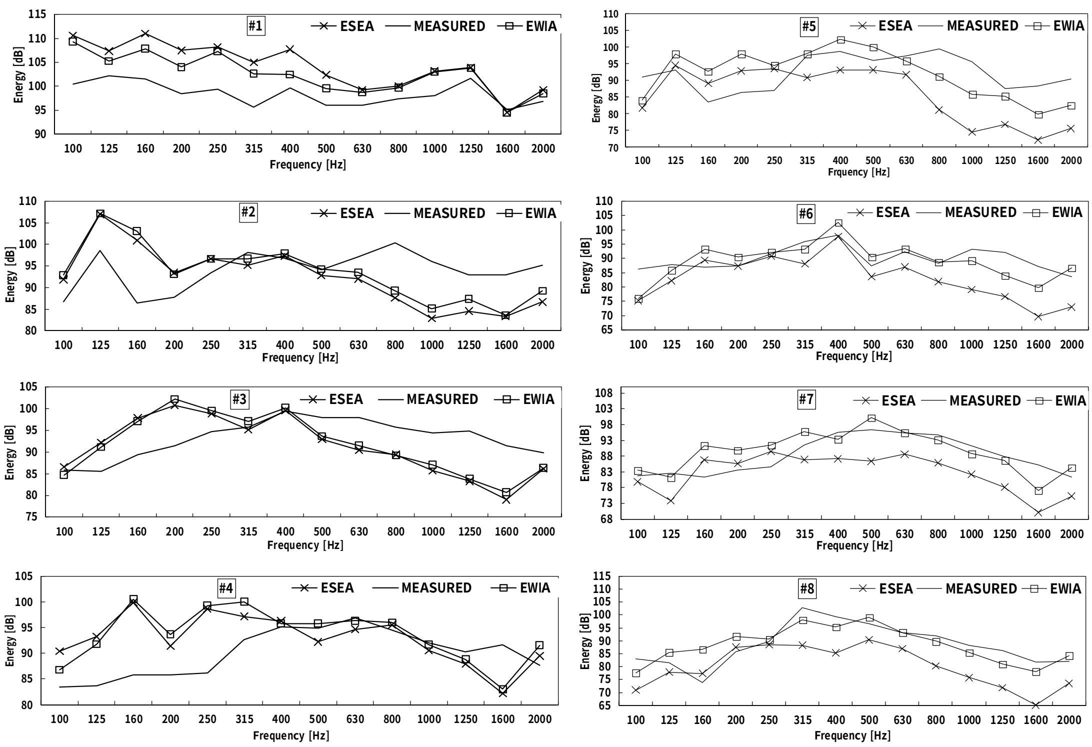


*Figure 5: Comparison between measured data, ESEA and EWIA for Dash-floor model*

## CONCLUSIONS

This paper presents a simplified experimental application of the WIA method, EWIA, proposed in ref.[3] which assumes theoretical distribution of the wave energy at boundaries between subsystems. It shows a comparison between the SEA, ESEA, WIA and EWIA methods based on their formulations and an application to a simple L-shape plate system. The results show that theoretical energy distribution at boundaries can be assumed for such systems and consequently EWIA can obtain good results using typical SEA experimental data obtained with the power injection method.

The method is then applied to a more complex system, which consists on a car dash-floor model. In this case SEA experimental data was also obtained through the power injection method and the results are compared with ESEA. These confirm that EWIA can improve ESEA results in the same way that WIA improves SEA results. Therefore, when subsystems present highly diffuse energy fields the results of ESEA and EWIA can be expected to be very close. On the other hand, as the distance between the subsystems and the energy input source increases the accuracy of the EWIA predictions also increases in comparison to ESEA. The reason is that increasing the number of boundaries between subsystems greatly affects the distribution of the energy field due to wave filtering and thus assuming non-diffuse energy field is more precise.

## REFERENCES

[1]. B.Cimerman, T.Bharj, G.Borello, “Overview of the Experimental Approach to Statistical Energy Analysis” Novem (1997).

[2]. H. Nishino, “Prediction of Medium Frequency Vibration by Wave Intensity Analysis” Novem (2000).

[3]. J.J.Bayod, T.Yamazaki & M.Kamata “Study on Prediction of Vibration Energy Levels of Structures using WIA based on Experimental Data”, Japanese Society Mechanical Engineering, acceptance pending (2006)

[4]. L.Cremer & M.Heckl, *Structure-Borne Sound*. (Springer-Verlag Berlin, Heidelberg, second edition, 1973 and 1988)

[5]. L. Wu, A. Agren & U. Sundback “A study of the initial decay rate of two-dimensional vibrating structures in relation to estimates of loss factor”, J. Sound and Vibration, **206(5)**, 663-684, (1997).

[6]. M. Petyt, *Introduction to Finite Element vibration Analysis*. (Cambridge Press 1990).

[7]. M. Wachulec, P.H. Kirkegaard, S. Nielsen, “Methods of Estimation of Structure Borne Noise in Structures–Review, “Structural Dynamics, Aalborg Univ, Paper No.20 (2000)

[8]. R.H. Lyon & R.G. DeJong, *Statistical Energy Analysis of Dynamic Systems: Theory and Applications*. (MIT Press, Cambridge, Second edition, 1975).

[9]. R.S. Langley, “A Wave Intensity Technique for the analysis of High Frequency Vibrations”, J. of Sound and Vibration, **159(3)**, 483-502 (1992).

[10]. R.S. Langley, “Wave Intensity Analysis of High Frequency Vibrations”, Philosophical Transactions of the Royal Society, **A346**, 489-499 (1994).

[11]. T.Yamazaki, M.Kamata & S.Ohno, “Practical Approach of Structural Intensity Meassurement Applied for Box-Like Structure”, Fifth International Congress on Sound and Vibrations 15-18 (1997).